# 5.3 W cw output power from a Master Oscillator Power Amplifier at 1083 nm

Bernd Sumpf [a], Sven Schwertfeger [a], Jörg Wiedmann [b], Andreas Klehr [a], Frank Dittmar [a], Götz Erbert [a], Günther Tränkle [a]
[a] Ferdinand-Braun-Institut für Höchstfrequenztechnik, Gustav-Kirchhoff-Straße 4, 12489 Berlin
[b] eagleyard Photonics GmbH, Rudower Chaussee 29 (IGZ), 12489 Berlin

## ABSTRACT

A master-oscillator power-amplifier system at $\lambda = 1083$ nm with 5.3 Watt output power and a narrow spectral linewidth was realised. The master oscillator was a distributed Bragg reflector (DBR) laser with a 3-µm wide ridge waveguide (RW) and a total length of 2 mm. The power amplifiers were a 4 mm long antireflection coated tapered laser diodes with 500 µm or 1000 µm long straight RW sections.
At a temperature of 40°C and an injection current of 160 mA, the DBR laser had a wavelength of 1083 nm. The emitted light of the DBR laser was focused into the tapered amplifier with a seed power of up to 36 mW. At 10°C and at a current through the tapered amplifier of 8.6 A, a maximum output power of 5.3 W was measured. Over the full operating range single longitudinal mode operation at a wavelength of $\lambda = 1083$ nm was maintained with a side mode suppression ratio better than 35 dB. The vertical far field angle was below 22° (FWHM).

**Keywords:** MOPA, DBR laser, tapered amplifier, high-power, diffraction limited radiation

## 1. INTRODUCTION

High brilliance, high power lasers are light sources which become more and more important not only for the pumping of solid state and fibre lasers and for non-linear frequency conversion, but also for medical applications.
There is an important application in the lung diagnostics using polarized helium. This application requires laser sources emitting at about 1083 nm with a spectral linewidth matched to the Doppler-width of the low pressure helium gas, i.e. about 2 GHz or 0.01 nm, a good beam quality, and an output power of 4 W. Up to now, Ytterbium-doped fibre lasers or Nd-doped lanthanum magnesium hexaluminate lasers were used for metastability-exchange optical pumping[1,2,3,4].
As an alternative semiconductor based laser systems are very attractive for this application, due to their smaller size and higher efficiency. A small spectral linewidth can be achieved by using distributed Bragg reflector (DBR) and distributed feedback (DFB) lasers. For $\lambda \approx 1083$ nm, Major and Welch[5] reported an output power of 220 mW and a wall-plug efficiency of about 27%. At $\lambda \approx 1062$ nm, Hofmann *et al.*[6] presented a maximum output power of 180 mW based on a structure described in Ref.[7]
Monolithically integrated semiconductor lasers, based on devices with an internal grating section and a flared amplifier are known for several wavelengths. For example, at 863 nm O'Brien *et al.*[8] reported 1.3 W output power with a side-mode suppression ratio of about 25 dB. For the wavelength range near 970 nm a maximum output power of 2 W was reported[9,10].
Another approach is the application of hybrid master-oscillator power-amplifier (MOPA) systems. The advantage of this solution is that the two devices can be independently controlled. The master oscillator, e.g. a DBR or DFB laser[11], can be tuned to the desired wavelength by varying temperature or current. Similarly, the operational conditions of the power amplifier, e.g. a tapered device, can be optimised towards maximum output power also by selecting an adequate temperature and current.
Highly anti-reflection coated broad area devices or tapered devices can be used as power amplifiers. The latter typically consist of a straight RW (ridge waveguide) section and a tapered gain section (like anti-reflection coated tapered lasers). Devices having only a tapered gain region (so called broad area flared amplifier) are known, too.

Optoelectronic Devices: Physics, Fabrication, and Application II, edited by Joachim Piprek,
Proc. of SPIE Vol. 6013 (SPIE, Bellingham, WA, 2005) · 0277-786X/05/$15 · doi: 10.1117/12.630640

At $\lambda$ = 860 nm, Goldberg *et al.*[12] presented the application of a broad area laser structure and obtained an output power of 3.3 W. At $\lambda \approx$ 970 nm the application of tapered devices were reported[13,14,15]. The highest diffraction limited output power of 5 W was obtained at this wavelength by O'Brien *et al.*[15]. The amplifier was a broad area flared device.

At an even longer wavelength at $\lambda$ = 1060 nm, our group[16] reported 3.1 W cw output power from a compact hybrid MOPA. The amplifier was an anti-reflection coated tapered laser.

With an $\alpha$-DFB Laser as master oscillator and a broad area device as amplifier up to 1.6 W maximal output power with nearly diffraction limited beam profile was obtained[17].

In this paper, we present the results for a hybrid MOPA using a 1083 nm DBR laser as master oscillator and an anti-reflection coated tapered laser as amplifier. Information on the manufacturing process, the power-current characteristic, and the spectral behaviour for the master oscillator and the tapered amplifier will be given. Then the design and the properties of the MOPA system will be described. The maximum output power, the dependence of the output power on the input power from the DBR laser, the spectral properties, and the beam characteristics will be given. The reached maximal output power is to the best of our knowledge the highest reported output power for a semiconductor based MOPA systems up to now.

## 2. THE DBR LASER

The master oscillator was a DBR laser consisting of gain, phase, and DBR section[11]. The layer structure was grown using two-step metalorganic vapour-phase epitaxy (MOVPE). The active region consists of a compressively strained InGaAs single quantum well embedded in tensile strained GaAsP spacer layers. The p- and n- doped GaAs waveguide layers are sandwiched between $Al_{0.25}Ga_{0.75}As$ cladding layers. For the p-contact a highly doped GaAs layer was grown. The first epitaxy ends with the p-GaAs waveguide layer. In this layer a first order grating with a period of 161 nm was formed in the DBR section by holographic photolithography with a He:Cd laser followed by wet chemical etching. Afterwards, the grating structure was overgrown in a second epitaxy step. The vertical far field angle of this layer structure is 30° (FWHM).

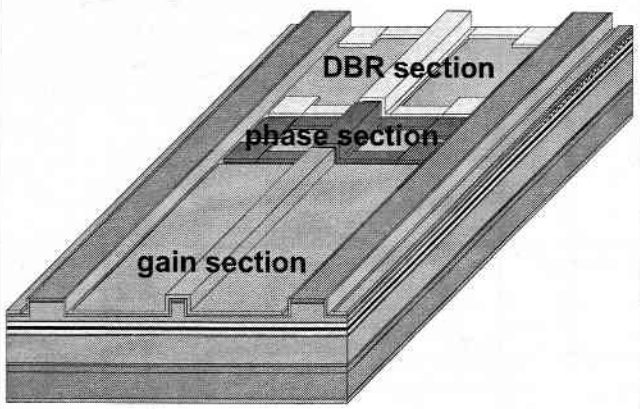


Figure 1: Schematic drawing of the three-section DBR laser

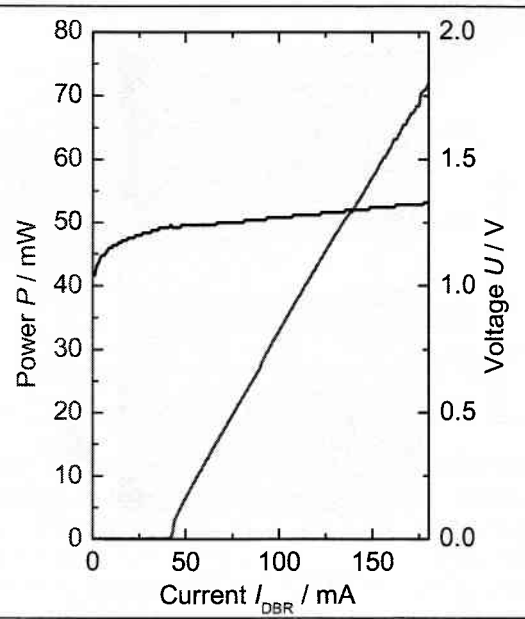


Figure 2: Power-voltage-current characteristics of the 1083 nm DBR laser at $T$ = 40°C

A scheme of the laser used in the experiments is shown in Fig 1. The lateral mode confinement is achieved with a RW having an effective index step of $\Delta n_{eff}$ = 0.005 and a ridge width of 3 µm. The total length of the laser is 2 mm;

the lengths of the single sections are 1000 µm, 500 µm, and 500 µm (gain, phase, DBR). The front- and back facets are coated to 10% and 0% reflectivity, respectively.
For measurements, the lasers are mounted p-side up on C-Mounts. The gain and phase section are connected in parallel. The required wavelength of $\lambda = 1083$ nm is reached at a temperature of 40°C. The power-voltage-current characteristic for the device used in the MOPA system is given in Fig. 2. The threshold current is $I_{th} = 42$ mA and the slope efficiency is 0.5 W/A. An output power of 50 mW is reached at 134 mA. The shift of the wavelength over the injection current is presented in Figure 3.

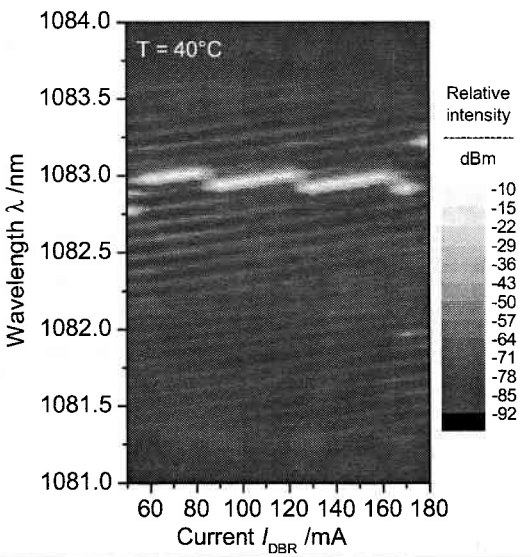


Figure 3: Spectral mapping of the DBR-laser at $T = 40$°C

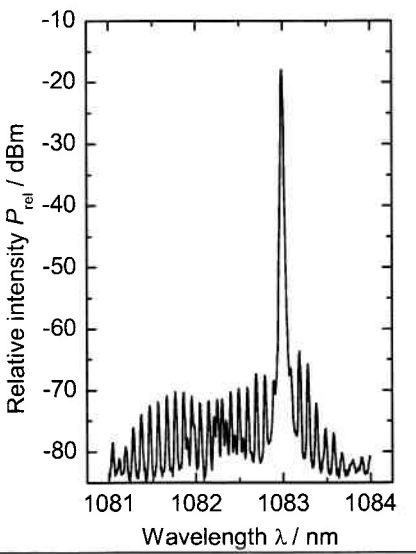


Figure 4: Spectrum of the DBR laser at $T = 40$°C for an excitation current of $I_{DBR} = 160$ mA

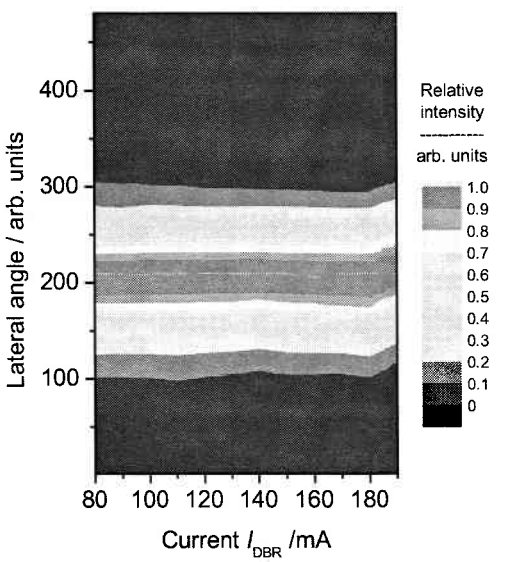


Figure 5: Lateral far field mapping of the DBR laser at $T = 40$°C

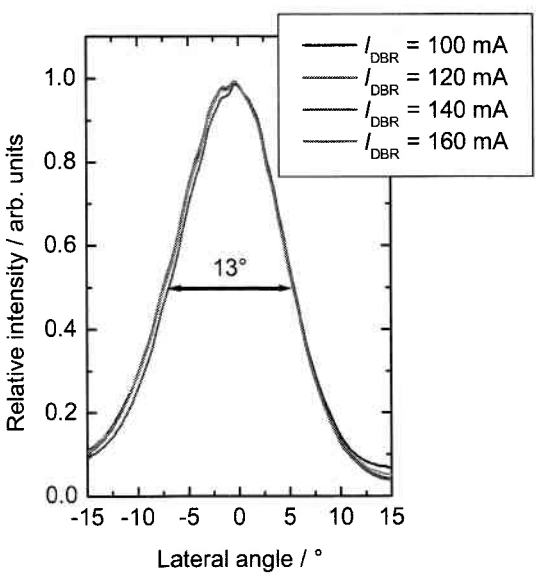


Figure 6: Lateral far field profiles of the DBR laser at $T = 40$°C for various injection currents

It can be seen that close to threshold two modes lase. If the current is larger than 60 mA, the wavelength increases with a tuning rate of about 0.002 nm/mA. At 90 mA, a hop towards the next smaller wavelength mode occurs, due to the thermal detuning of the grating and gain section. At higher currents the wavelength increases again until the next

mode hop. At currents larger than 160 mA, which corresponds to output powers larger than 65 mW the laser operates multi-mode. The spectrum for an injection current of $I_{DBR}$ = 160 mA ($P$ = 65 mW) is shown in Fig. 4. It can be seen that the side mode suppression ratio is better than 40 dB.
The lateral far field was also measured as a function of the injection current. Fig. 5 shows such a lateral far field mapping measured at 40°C. The colours represent the measured relative intensities. In the range from 80 mA to 180 mA the far field profiles do not exhibit any no beam steering. This is important for the stable coupling of the emitted radiation from this master oscillator into the power amplifier. In Fig. 6 the lateral far field profiles in the current range 100 mA ≤ $I_{DBR}$ ≤ 160 mA, are presented. The lateral far field width is 13° (FWHM).
With these spectral and spatial features the DBR laser is suitable for the application in the MOPA system for 1083 nm.

## 3. THE TAPERED AMPLIFIER

The epitaxial layers for the tapered device were also grown by low pressure MOVPE. The active layer is formed by an InGaAs double quantum well embedded in a 3.6 µm thick $Al_{0.25}Ga_{0.75}As$ waveguide layer and $Al_{0.50}Ga_{0.50}As$ cladding layers. The layer sequence is completed by a highly doped p-GaAs contact layer. The very broad waveguide layer leads to a narrow vertical far field as shown in Fig 7. The full width half maximum is 22° and 95% of the energy is emitted within an angle smaller than 38°. The design of comparable structures for 808 nm was recently described in Ref.[18]

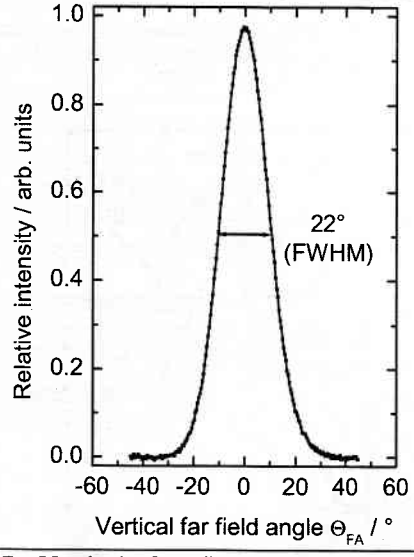


Figure 7: Vertical far field angle of the tapered amplifier

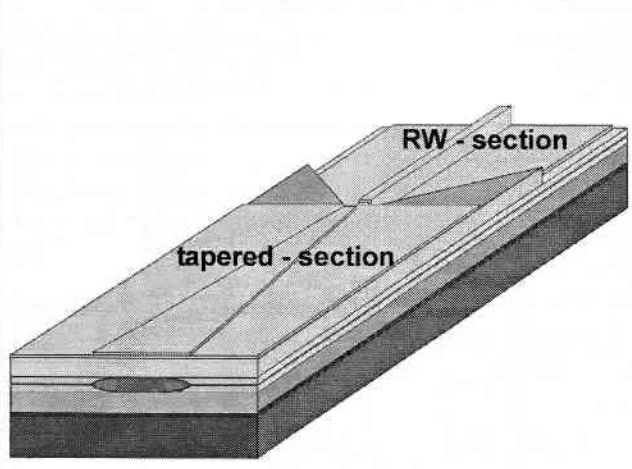


Figure 8: Schematic drawing of the tapered amplifier

In Fig. 8, a scheme of the tapered amplifier used in the experiment is given. The device consists of an index-guided straight section and a gain-guided tapered section. The index guiding is achieved by a RW formed by reactive ion etching and the deposition of an insulator on the etched surface. The ridge width is $W_{RW}$ = 3 µm. In the tapered section, the contact layer outside of the p-electrode was removed by wet chemical etching in order to reduce current spreading. The metallization on the p-side contact was formed by evaporating a Ti-Pt-Au multilayer and by electro-plating a thick Au layer. After thinning and n-metallization the wafer was cleaved to a total cavity length of $L$ = 4 mm. The devices used in the experiments have a total taper angle of $\varphi_{TR}$ = 6° and different lengths of the ridge waveguide section of $L_{RW}$ = 500 µm and 1000 µm, respectively. The length $L_{RW}$ and the full angle $\varphi_{TR}$ of the tapered section were selected based on results for other wavelengths[19,20].

The front and the rear facets were anti-reflection coated ($R \leq 5\times10^{-4}$). The devices were mounted p-side (epi-side) down on CuW submounts using AuSn[21]. This subassembly was soldered on C-mounts using PbSn. The n-side was contacted by wire bonding.

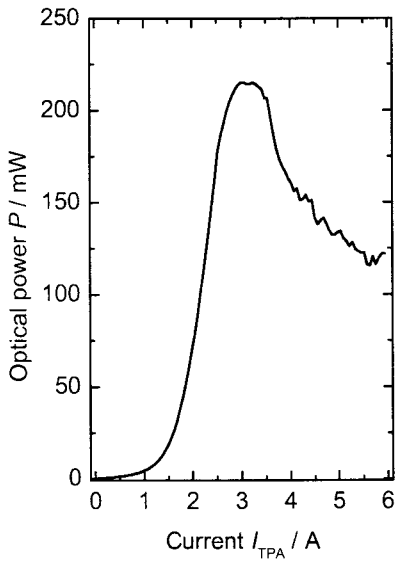


Figure 9: Power-current characteristics for the tapered amplifier with $L_{RW}$ = 500 µm at $T$ = 10°C

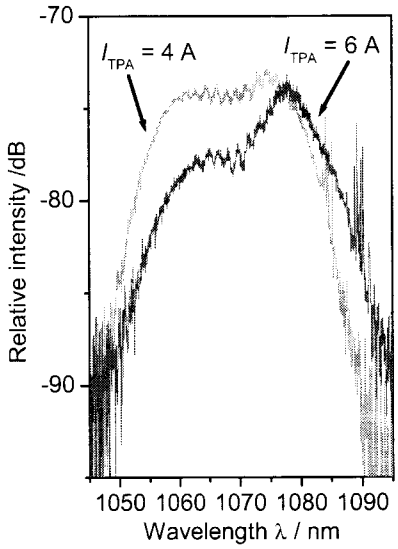


Figure 10: Spectra for the tapered amplifier with $L_{RW}$ = 500 µm at $T$ = 10°C

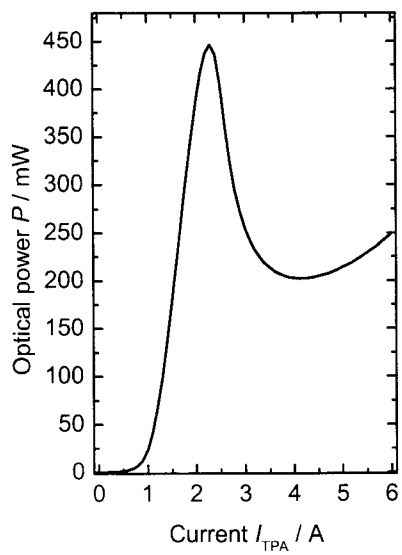


Figure 11: Power-current characteristics for the tapered amplifier with $L_{RW}$ = 1000 µm at $T$ = 10°C

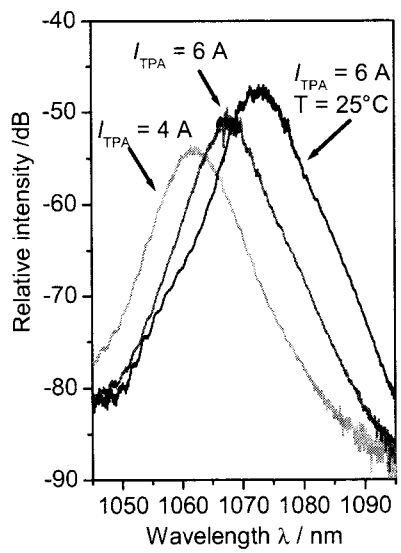


Figure 12: Spectra for the tapered amplifier with $L_{RW}$ = 1000 µm at $T$ = 10°C and $I_{TPA}$ = 4 A and 6 A and $T$ = 25°C and $I_{TPA}$ = 6 A.

For these devices the power-current characteristics and the spectra of the amplified spontaneous emission (ASE) were measured. From Fig. 9, it can be seen that the device with $L_{RW}$ = 500 µm reaches at about $I_{TPA}$ = 3 A a maximum output power of about 220 mW. The output power decreases down to 125 mW at $I_{TPA}$ = 6 A. In Figure 10, the ASE spectra of this device is given for $I_{TPA}$ = 4 A and $I_{TPA}$ = 6 A. It can be seen, that at 4 A the spectral bandwidth is between 1050 and 1086 nm (measured for 95% (13 dB) power decrease). At $I_{TPA}$ = 6 A the wavelength shifts to longer values as expected, the spectral bandwidth is between 1051 nm and 1091 nm.

The same measurement was performed for the device with a ridge length of 1000 µm. In this case the output power reaches a higher maximum value of $P$ = 450 mW at $I_{TPA}$ = 2.3 A and also a decrease of the power for higher currents is observed as shown in Figure 11. The spectral bandwidth given in Figure 12 is smaller compared to the device with the shorter ridge waveguide section. At $T$ = 10°C and $I_{TPA}$ = 4 A, it covers the range from 1053 nm up to 1072 nm. At $I_{TPA}$ = 6 A the spectral bandwidth is between 1069 nm and 1077 nm at 10°C and in the range 1064 nm up to 1084 nm at 25°C.
For a high power operation of the MOPA system a low operation temperature of the power amplifier is favourable. But, the best overlap between master oscillator and power amplifier is obtained if the power amplifier operates at T = 25°C. Therefore using the tapered amplifier in the MOPA system, a compromise concerning temperature and spectral overlap is necessary.

## 4. THE HYBRID MASTER OSCILLATOR POWER AMPLIFIER

The experimental set-up for the hybrid master oscillator power amplifier system is given in Fig. 13. The master oscillator is placed on a heat sink, which can be adjusted to temperatures between 10°C and 70°C with an accuracy of 0.02 K. The DBR laser is driven with currents up to $I_{DBR}$ = 160 mA (i.e. $P_{seed}$ = 36 mW) with an accuracy of $\Delta I_{DBR}$ = 1 mA. The emitted radiation of the DBR laser is focussed via lenses $L_1$ and $L_2$ into the power amplifier. Lenses $L_1$ and $L_2$ are identical aspheres with a focal length of 8 mm. A 60 dB Faraday isolator is implemented between lenses $L_1$ and $L_2$ to prevent that light emitted from the rear side of the power amplifier travels back and couples into the DBR laser. The tapered amplifier is mounted on a heat sink capable to remove up to 55 W of heat.
The light from the tapered amplifier is collimated with lens $L_3$, which is of the same type as the other two lenses. With an integrating sphere the power-current characteristics is measured. The emission spectra are measured with a spectrum analyser (ADVANTEST Q8384) with a resolution of $\Delta\lambda$ = 0.01 nm. All measurements are computer controlled.
The position of the beam waist and the intensity profiles in the beam waist, at the front facet and in the far field were measured applying the method of the moving slit (DIN/ISO 11146, Annex A). Based on the measured intensity profiles, the beam propagation factor $M^2$ was calculated. The beam widths needed to calculate $M^2$ were identified with the $1/e^2$ widths of the intensity profiles in the beam waist and in the far field. The experimental details of the laser beam analyser set-up were discussed by Hülsewede *et al.*[22]

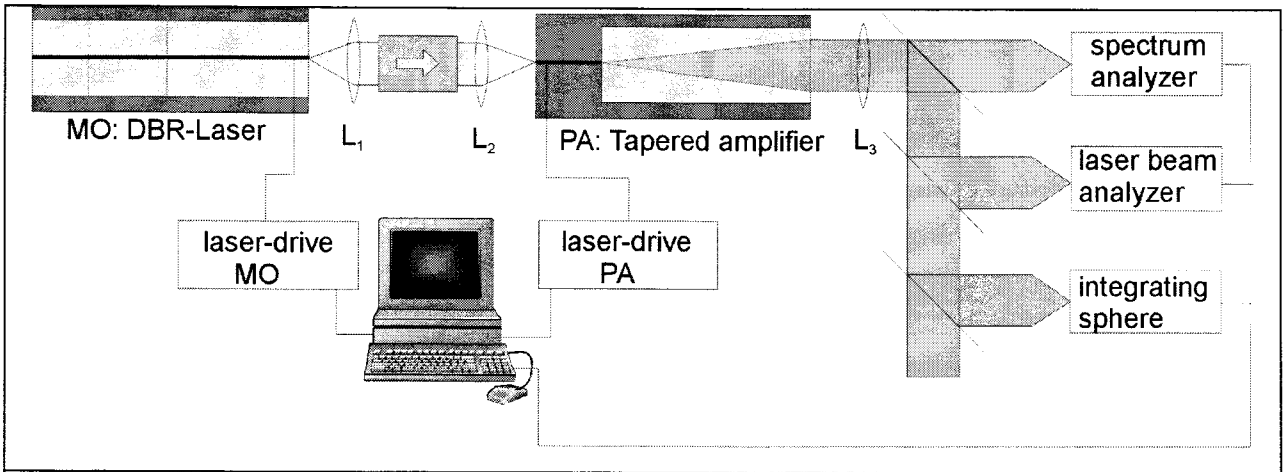


Figure 13: Scheme of the experimental set-up of the MOPA system

### 4.1. MOPA system with tapered device with $L_{RW}$ = 500 µm

The measured power-current characteristic for the MOPA system for several output powers of the DBR laser is given in Fig. 14. The temperature was reduced down to $T$ = 10°C to obtain high output power for excitation currents of $I_{TPA}$ > 8 A. The current of the DBR laser was adjusted to have a focused power on the rear side of the tapered

amplifier, the so called seed power $P_{seed}$, of 7 mW, 13 mW, 25 mW and 36 mW, respectively. This seed power is by a factor of 0.6 smaller compared to the power emitted from the DBR laser. The power loss can be attributed due to the cut-off of the beam by the small aperture of the optical isolator. For the largest seed power of $P_{seed}$ = 36 mW at an excitation current of $I_{TPA}$ = 8.6 A the maximum output power of $P$ = 5.3 W was measured. This is to the best of our knowledge the highest output power measured for such a MOPA system. The amplification of the light starts for a $P_{seed}$ = 36 mW at $I_{TPA}$ = 1.5 A, which corresponds to a current density of 230 A/cm$^2$. The slope efficiency is 0.88 W/A. It can be seen that with increased seed power within the studied range, the output power of the MOPA for a constant current $I_{TPA}$ increases too.

For various seed powers and amplifier currents the spectra of the MOPA were measured. All spectra showed single mode emission. To illustrate this, in Fig. 15, the spectrum for $I_{TPA}$ = 8 A, which corresponds to an output power of 4.9 W, is shown. The side mode suppression ratio is about 36 dB. This value is only slightly smaller than the value of the DBR laser (40 dB).

The beam quality for the MOPA was measured, for best results, with a seed power of $P_{seed}$ = 25 mW. The beam waists for different output powers are given in Fig. 16. At small output power $P \leq 2$ W the beam waist is smaller than 12 µm. The power in the central lobe is larger than 70% and the side lobes are weak. The beam propagation ratio is $M^2 \leq 3$.

At output powers $P \geq 3$ W the side lobes become more pronounced and the beam waist increases. In our experiment, the value raised up to 26 µm at $P$ = 4.5 W. The beam propagation ratio is still below 5 and about 60% of the power is in the central lobe.

In Fig. 17 the measurement of the near field at various output powers of $P$ = 2, 3 and 4 W with a seed power of $P_{seed}$ = 25 mW is presented. For low currents up to 3 A the near field width is about 390 µm and slightly larger than the manufactured output aperture of 370 µm. At currents larger than 3 A the near field begins to narrow down to 335 µm at $I_{TPA}$ = 4.5 A. The far fields, which were measured under the same conditions, are shown in Fig. 18. The far field width starts for low currents at about 17°. Then the far field width becomes smaller with increasing output power. The beam parameters for this MOPA set-up are compiled in Table 1.

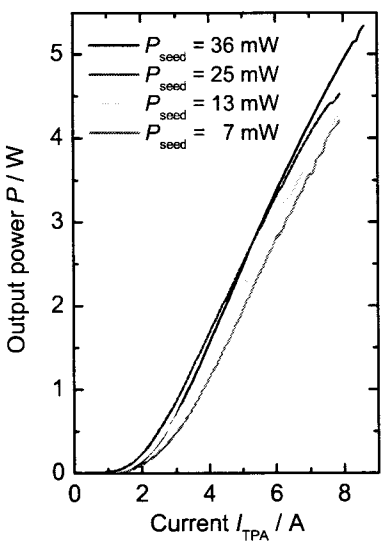


Figure 14: Power-current characteristics for the MOPA system using the tapered amplifier with $L_{RW}$ = 500 µm at $T$ = 10°C. The seed power from the DBR-laser is used as parameter.

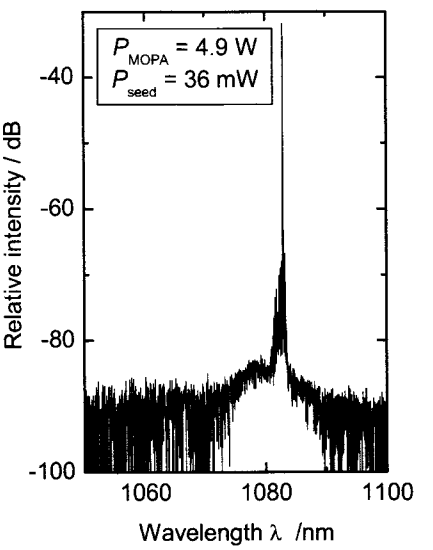


Figure 15: Spectrum for the MOPA system using the tapered amplifier with $L_{RW}$ = 500 µm at $T$ = 10°C.

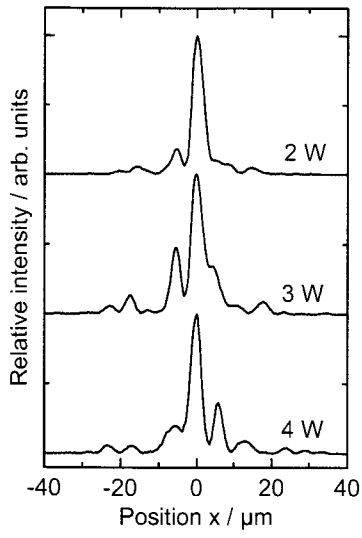


Figure 16: Beam waist measurement for the MOPA system using the tapered amplifier with $L_{RW}$ = 500 µm at $T$ = 10°C.

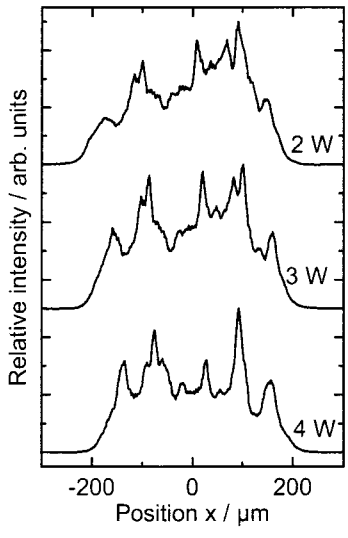


Figure 17: Near field measurement for the MOPA system using the tapered amplifier with $L_{RW}$ = 500 µm at $T$ = 10°C.

The behaviour of the beam waist is also typical for tapered lasers without beam spoilers. At small output powers the filtering of the radiation in the RW section is sufficient and on the other hand at high output powers side modes appear. This can be controlled by a proper adjustment of the length of the RW[19]. To prove this the experiments with a tapered amplifier with a RW length of 1000 µm were performed.

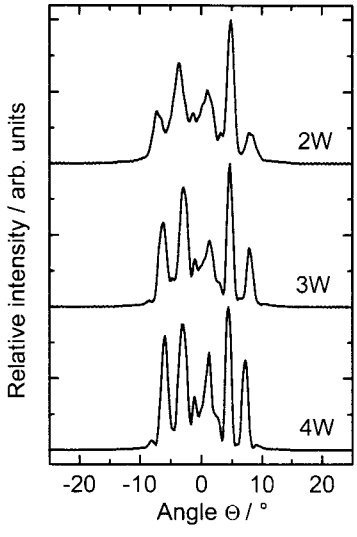


Figure 18: Far field measurement for the MOPA system using the tapered amplifier with $L_{RW}$ = 500 µm at $T$ = 10°C. The seed power is 25 mW.

*Table 1: Beam parameter for the MOPA system with $L_{RW}$ = 500 µm, $P_{seed}$ = 25 mW*

| Output power | Beam waist | Far field width | $M^2$ | Near field width | Power in main lobe | Astigmatism |
|---|---|---|---|---|---|---|
| W | µm | ° | | µm | % | µm |
| 1 | 11.1 | 18.0 | 2.5 | 389 | 72 | 1125 |
| 2 | 10.0 | 17.2 | 2.2 | 388 | 74 | 1160 |
| 3 | 24.6 | 16.2 | 5.0 | 385 | 65 | 1205 |
| 4 | 15.8 | 15.1 | 3.0 | 363 | 54 | 1210 |
| 4.5 | 26.1 | 13.2 | 4.4 | 335 | 61 | 1180 |

### 4.2. MOPA system with tapered device with $L_{RW}$ = 1000 µm

Firstly, the measurements were performed at $T$ = 25°C to guarantee a better spectral overlap between the emission wavelength of the DBR laser and the gain region of the tapered amplifier in the full current range. The measured power-current characteristic for the MOPA system with the power amplifier with longer ridge waveguide section $L_{RW}$ = 1000 µm is shown in Fig. 19. Again the measurements were performed for different seed powers. It can be seen that the power-current-characteristic is rather linear and comparable to the measured characteristic for the device with the shorter $L_{RW}$ = 500 µm (see Fig. 14). For the largest seed power of $P_{seed}$ = 36 mW an output power of 5.1 W for an amplifier current of 8 A was achieved. In addition the slope efficiency was also 0.89 W/A.

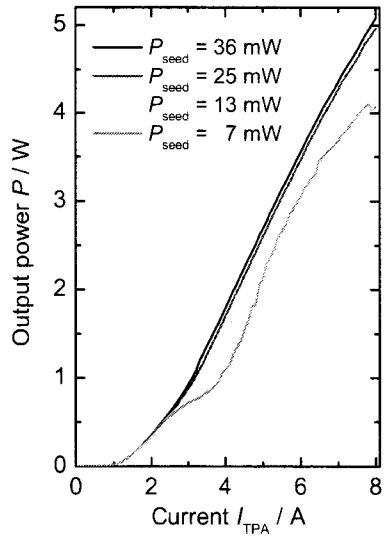


Figure 19: Power-current characteristics for the MOPA system using the tapered amplifier with $L_{RW}$ = 1000 µm at $T$ = 25°C. The seed power is used as parameter.

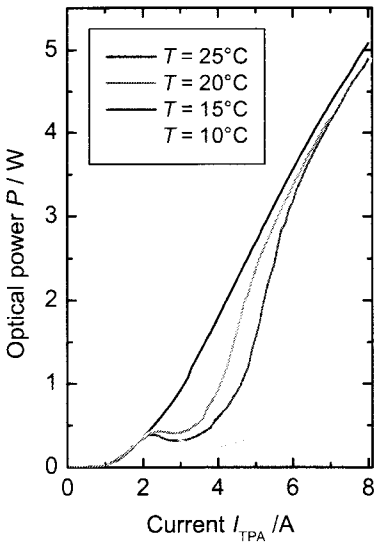


Figure 20: Power-current characteristics or the MOPA system using the tapered amplifier with $L_{RW}$ = 1000 µm and $P_{seed}$ = 36 mW. The temperature is used as parameter.

To study the influence of the insufficient spectral overlap between DBR-laser and gain region of the tapered device, the power current characteristics at different temperatures were measured. In Fig. 20, the power-current characteristics for different temperatures $T$ = 10°C, 15°C, 20°C, and 25°C are shown. At lower temperature the amplification of the seed power starts only at higher currents. The reason for this behaviour is that only at the higher current the gain region matches to the wavelength of the DBR-laser. Only if the tapered device has sufficient gain at 1083 nm the amplification takes places. For example, at $T$ = 10°C the shape of the power-current-characteristics up to 4 A is similar to the characteristics of the unseeded device as shown in Fig. 11.

The optimum between output power and beam quality was found for a temperature of $T = 15°C$. Therefore all further measurements were performed at this temperature.

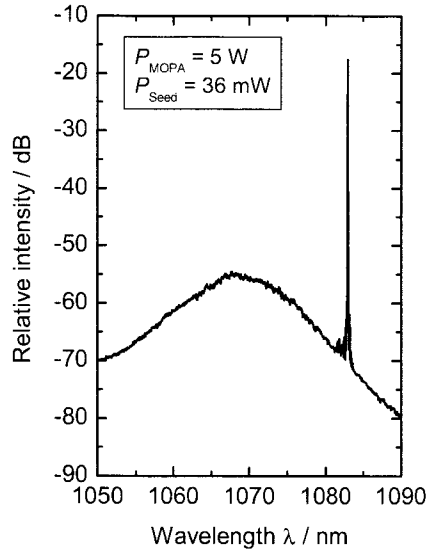


Figure 21: Spectrum for the MOPA system using the tapered amplifier with $L_{RW} = 1000$ µm at $T = 15°C$.

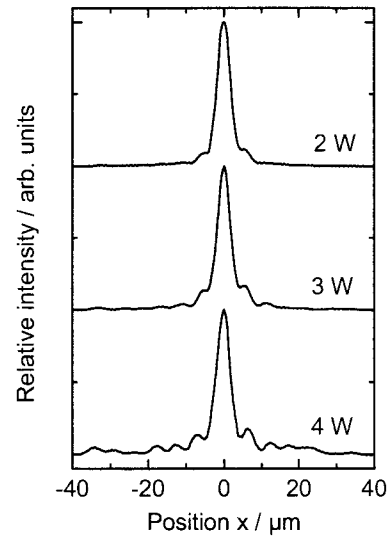


Figure 22: Beam waist measurement for the MOPA system using the tapered amplifier with $L_{RW} = 1000$ µm at $T = 15°C$. The seed power is 25 mW.

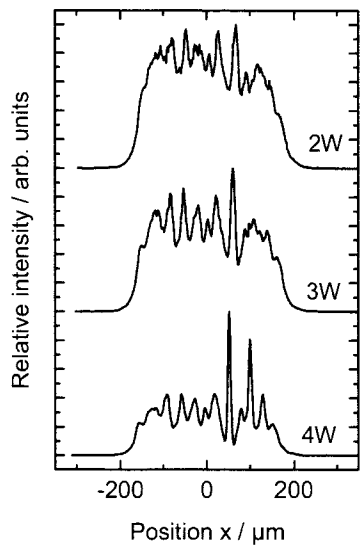


Figure 23: Near field measurement for the MOPA system using the tapered amplifier with $L_{RW} = 1000$ µm at $T = 15°C$. $P_{seed} = 25$ mW

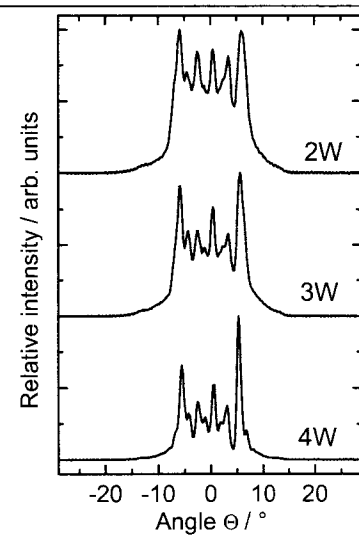


Figure 24: Far field measurement for the MOPA system using the tapered amplifier with $L_{RW} = 1000$ µm at $T = 15°C$. $P_{seed} = 25$ mW

The spectrum was measured for an output power of 5 W ($I_{TPA} = 8$ A, $P_{seed} = 36$ mW). As shown in Figure 21, the side mode suppression ratio (SMSR) improved, compared to the first device with the shorter RW section, to about 40 dB, which is now the same as that of the DBR-laser.

Figure 22 showed the measured beam waist for an output power between 2 W and 4 W. As expected for the device with the longer RW section, the beam quality is improved. The width of the beam waist is over the complete power

range rather constant and smaller than 12 µm. This is an improvement compared to the device with the shorter RW section ($L_{RW}$ = 500 µm). The beam propagation ration is with $M^2$ = 2.6 at 4 W also significantly smaller. For all output powers the power in the central lobe is larger than 64%.
From Fig. 23 and 24 the improved shape of the near field and far field can be observed. The near field is less structured and had a top hat profile and also the far field is significantly less structured. The near field width for this device is also larger compared to the manufactured output aperture of about 320 µm.
The beam parameters for the power amplifier with the longer ridge waveguide section are summarized in Table 2.

*Table 2: Beam parameter for the MOPA system with $L_{RW}$ = 1000 µm, $P_{seed}$ = 25 mW, T = 15°C*

| Output power | Beam waist | Far field width | $M^2$ | Near field width | Power in main lobe | Astigmatism |
|---|---|---|---|---|---|---|
| W | µm | ° | | µm | % | µm |
| 2 | 7.6 | 18.5 | 1.8 | 355 | 85 | 1050 |
| 3 | 11.9 | 17.2 | 2.6 | 351 | 74 | 1080 |
| 4 | 11.8 | 14.4 | 2.1 | 329 | 64 | 1120 |

The observed differences for the two different power amplifiers are comparable to corresponding results for tapered lasers. In tapered lasers the length of the ridge waveguide determines the filtering of the back travelling radiation. If the RW is too short, back reflected light from the front facet could reach the rear facet even outside the ridge and can than again reach the tapered section, where the light is amplified[23]. In the case of a tapered amplifier the principal mechanism is similar. Light, which was not coupled directly into the ridge, but passed to the left and to the right of the ridge can travel through a very short ridge section and will nevertheless be amplified in the flared section. In both cases a certain minimal length of the RW section is necessary for the proper filtering and suppression mechanism to obtain a nearly diffraction limited beam shape.

## 5. SUMMARY AND OUTLOOK

The properties of a hybrid master-oscillator power-amplifier system for the wavelength at 1083 nm were studied. Two power amplifiers with different lengths of the ridge waveguide section were tested. The maximum output power of both devices was comparable. A record large output power of 5.3 W was achieved. For a device with a ridge waveguide of 1000 µm up to an output power of 4 W the beam shape was diffraction limited. The beam propagation ratio at $P$ = 4 W was $M^2$ = 2.1.
After this successful development a further improvement of the beam quality with by adjusting the effective index-step in the RW section and an investigation of devices with different taper angles are promising. Moreover, even larger output powers can be expected by further adjustment of the spectral gain peak of the amplifier and it's tuning relative to the wavelength of the seed laser as well as by increasing the total length of the devices.

## Acknowledgments

The authors gratefully acknowledge J. Hopp and P. Brade for technical support.

## REFERENCES


1. T. R. Gentile, M. E. Hayden, M. J. Barlow, Comparison of metastability-exchange optical pumping sources, *J. Opt. Coc. Am. B* 20, 2068-2074 (2003)
2. G. Tastevin, S. Grot, E. Courtade, S. Bordais, P.-J. Nacher, A broadband Ytterbium-doped tunable fiber laser for $^3$He optical pumping at 1083 nm; *Appl. Phys. B* 78, 145-156 (2004)
3. T. R. Gentile, D. R. Rich, A. K. Thompson, W. M. Snow, G. L. Jones, Compressing Spin-Polarized $^3$He with a modified diaphragm pump; *J. Res. Natl. Inst. Stand, Technol.* 106, 709-729 (2001)
4. D. S. Hussey, D. R. Rich, A. S. Below, X. Tong, H. Yang, C. Bailey, C- D- Keith, J. Hartfield, G. D. R. Hall, T. C. Black, W. M. Snow, T. R. Gentile, W. C. Chen, G. L. Jones, E. Wildman, Polarized $^3$He gas compression system using metastability-exchange optical pumping, *Rev. Sci. Instrum.* 76, 053503 (2005)
5. J. S. Major Jr., D. F. Welch, Singlemode inGaAs/GaAs distributed Bragg reflector laser diodes operating at 1083 nm, *Electronics Letters*, 29, 2121-2122 (1993)
6. L. Hofmann, A. Klehr, F. Bugge, H. Wenzel, V. Smirnitski, J. Sebastian, G. Erbert, 180 mW DBR lasers with first-order grating in GaAs emitting at 1062 nm, *Electronics Letters*, 36, 534-535 (2000)
7. F. Bugge, A. Knauer, U. Zeimer, J. Sebastian, V. B. Smirnitski, A. Klehr, G. Erbert, M. Weyers, MOVPE grpeoth of tunable DBR laser diode emitting at 1060 nm, *J. Cryst. Growth,* 195, 676-680 (1998)
8. S. O'Brien, D. Mehuys, J. Major, R. Lang, R. Parke, D. F. Welch, D. Scifres, 1.3 W CW, diffraction-limited monolithically integrated master oscillator flared amplifier at 863 nm, *Electronics Letters* 29, 2109-2110 (1993)
9. R. Parke, D. F. Welch, A. Hardy, R. Lang, D. Mehuys, S. O'Brian, K. Dzurko, D. Scifres, 2.0 W cw, diffraction-limited operation of a monolithically integrated master oscillator power amplifier, *IEEE Photonics technology letters* 5, 297-300 (1993)
10. S. O'Brien, D. F. Welch, R. A. Parke, D. Mehuys, K. Dzurko, R. J. Lang, R. Waarts, D. Scifres, Operating Characteristics of a high-power monolithically integrated flared amplifier master oscillator power amplifier, *IEEE Journal of Quantum Electronics* 29, 2052-2057 (1993)
11. M. C. Amann, J. Buus, Tunable Laser Diodes (Artech House, Norwood, 1998)
12. L. Goldberg, D. Mehuys, D. C. Hall, 3.3 W cw diffraction limited broad area semiconductor amplifier, *Electronics Letters* 28 1082-1084 (1992)
13. J. N. Walpole, E. S. Kintzer, S. R. Chinn, C. A. Wang, L. J. Missaggia, High-power strained-layer InGaAs/AlGaAs tapered traveling wave amplifier, *Applied Physics Letters* 61, 740-742 (1992)
14. E. S. Kintzer, J. N. Walpole, S. R. Chinn, C. A. Wang, L. J. Missaggia, High-power, strained-layer amplifiers and lasers with tapered gain regions, *IEEE Photonics Technology Letters* 5, 605- 608 (1993)
15. S. O'Brien, A. Schoenfelder, R. J. Lang, 5 W cw diffraction-limited InGaAs broad-area flared amplifier at 970 nm, *IEEE Photonics Technology Letters* 9, 1217-1219 (1997)
16. S. Schwertfeger, A. Klehr, G. Erbert, G. Tränkle, Compact hybrid master oscillator power amplifier with 3.1 W cw output power at wavelength around 1061 nm, *IEEE Photonics Technology Letters* 16, 1268-1270 (2004)
17. K. Paschke, T. Reiche, G. Erbert, R. Güther, J. Fricke, F. Bugge, J. Sebastian, 1.6 W hybrid master oscillator power amplifier with α-DFB-laser as master oscillator at 1057 nm, *Electronics Letters* 38, 321-322 (2002)
18. A. Knauer, G. Erbert, R. Staske, B. Sumpf, H. Wenzel, M. Weyers, High-power 808-nm lasers with a super-large optical cavity, *Semicond. Sci. Technol.* 20, 621–624 (2005)
19. B. Sumpf, R. Hülsewede, G. Erbert, C. Dzionk, J. Fricke, A. Knauer, W. Pittroff, P. Ressel, J. Sebastian, H. Wenzel, G. Tränkle, High Brightness 735 nm Tapered Lasers - Optimisation of the Laser Geometry, *Optical and Quantum Electronics* 35, 521-532 (2003)
20. H. Wenzel, B. Sumpf, G. Erbert, High-brightness diode lasers, *Comptes Rendus Physique* 4, 649-661 (2003)
21. W. Pittroff, G. Erbert, G. Beister, F. Bugge, A. Klein, A. Knauer, J. Maege, P. Ressel, J. Sebastian, R. Staske, G. Tränkle, Mounting of high power laser diodes on boron nitride heat sinks using an optimised Au/Sn metallurgy, *IEEE Transactions on Advanced Packaging* 24, 434–441 (2001)
22. R. Hülsewede, J. Sebastian, H. Wenzel, G. Beister, A. Knauer, G. Erbert, Beam quality of high power 800 nm broad-area laser diodes with 1 and 2 μm long optical cavity structures, *Optics Communication* 192, 69-75 (2001)
23. L. Borruel, S. Sujecki, M. Krakowski, B. Sumpf, P. Moreno, J. Wykes, S. C. Auzanneau, G. Erbert, D. Rodríguez, P. Sewell, M. Calligaro, H. Wenzel, T. M. Benson, E. C. Larkins, I. Esquivias; High brightness tapered lasers at 732 nm and 975 nm: experiments and numerical analysis, *Conf. Dig. IEEE 18th Int. Semiconductor Laser Conf.,* Garmisch Partenkirchen, Germany, 89–90 (2002)